Role of Chain Connectivity across an Interface on the Dynamics of a Nanostructured Block Copolymer

Dane Christie, Richard A. Register, and Rodney D. Priestley

Phys. Rev. Lett. **121**, 247801 — Published 12 December 2018

DOI: 10.1103/PhysRevLett.121.247801

The Role of Chain Connectivity Across an Interface on the Dynamics of a Nanostructured Block Copolymer

Dane Christie[1], Richard A. Register[1,2*], and Rodney D. Priestley[1,2*]

[1]Department of Chemical and Biological Engineering

[2]Princeton Institute for the Science and Technology of Materials

Princeton University

Princeton, New Jersey 08544 USA

***Correspondence to:** register@princeton.edu and rpriestl@princeton.edu

Abstract: Fluorescence labeling enables component- and location-specific measurements of the glass transition temperature (T_g) in complex polymer systems. Here we characterize the T_g of fluorescently-labeled poly(methyl methacrylate) homopolymers, PMMA-py, blended at low concentrations into an unlabeled lamellar poly(n-butyl methacrylate-b-methyl methacrylate) diblock copolymer, PBMA-PMMA. In this system the PMMA-py homopolymer is sequestered within the PMMA domains of the diblock copolymer and subject to soft confinement by the domains of the lower-T_g PBMA block, which lowers the homopolymer T_g by ~5K beyond the contribution of segmental mixing. In contrast to the PMMA block in the diblock copolymer, the PMMA-py homopolymer is not covalently bound to the interdomain interface. A comparison of T_g for the homopolymers in the blends to T_g for diblock copolymers with equivalent labeled segment density profiles reveals that the homopolymer's T_g is consistently ~10 K higher than for diblock segments at the same location within the domain structure, highlighting the dominant contribution of a covalent bond across the interface to the perturbation of the chain dynamics in the block copolymer.

Main text: The presence of chemical heterogeneity in a single polymer chain underpins the scientific and technological relevance of diblock copolymers. In sufficiently long diblock copolymer chains, wherein the interactions between dissimilar (A and B) segments are repulsive, the dissimilar blocks separate from each other over the length scale of the polymer chain [1,2], yielding periodic domains of order 10 - 100 nm enriched in one segment type, divided by internal interfaces. Local mixing between the two blocks still occurs, such that each segment type has a concentration profile that

varies continuously across the domain period, from being rich in A to rich in B. Nanostructured diblock copolymers present excellent systems to investigate the relationships between nanoscale confinement, segmental mixing, the confining interfaces, and the glass transition temperature (T_g). The parameters governing the domain T_g—namely, the bulk T_g of the A and B homopolymers, the confinement length scale, the degree of segmental mixing, and the interfacial thickness—can be systematically varied by choosing the block chemistries and total chain length. Blends of block copolymers and their constituent homopolymers offer an experimental system wherein polymer chains exist under similar confinement conditions as the neat diblock copolymer, with the difference being the lack of attachment of the homopolymer to the interface [3-6]. Provided that a characterization tool which enables component-specific measurements of T_g is utilized, the effect of chain connectivity across the domain interface can be unambiguously quantified.

Even in miscible polymer blends, the dynamics of a component cannot be described by the blend-averaged value if the components are weakly interacting and have a large dynamic contrast, i.e., a large difference in bulk T_g [7-11]. The dynamics of a component in the blend can be understood through the phenomenon of self-concentration described by Lodge and McLeish [12]: in the neighborhood of an A segment, within a volume defined approximately by the cube of a Kuhn length, the segmental concentration of A is elevated relative to its average value in the blend due to chain connectivity, biasing the individual component dynamics towards those of the pure component [13,14]. In nanostructured diblock copolymers with a large T_g contrast, there are thus contributions to dynamical heterogeneity which are operative over

different length scales [15,16]. At the length scale of a Kuhn segment, local mixing between the blocks acts to perturb a component's T_g in a similar manner to miscible polymer blends. At the length scale of the domain period (*d*), the high- and low-T_g blocks exist under soft and hard confinement conditions, respectively. Under soft confinement, a polymer's T_g will be depressed relative to bulk [17,18].

Previously [19], we characterized the component dynamics of a nanostructured block copolymer with a large T_g contrast via the incorporation of a fluorescent monomer at selected positions along the chain, interrogated via temperature-dependent fluorescence spectroscopy. In this Letter, we advance the understanding of soft confinement on T_g by quantifying the depression attributable to the connectivity of the block across the domain interface. The experimental system consists of blends of a lamellar poly(n-butyl methacrylate-*b*-methyl methacrylate) diblock copolymer, PBMA-PMMA, with 2 vol% of a pyrene-labeled poly(methyl methacrylate) homopolymer, PMMA-py. The homopolymers span a molecular weight (M) range of 8.4 - 69 kg/mol, each with a labeling level of <0.5 mol%. The T_g contrast in this system is 96 K; PMMA is the high-T_g component. Comparing the cases where the fluorescent label resides on the PMMA homopolymer vs. on the PMMA block of the diblock copolymer reveals that attachment of the PMMA block to the PBMA block (and thereby to the domain interface) produces the principal reduction in T_g—larger than that resulting from segmental mixing, or from confining the homopolymer within the block copolymer domain structure.

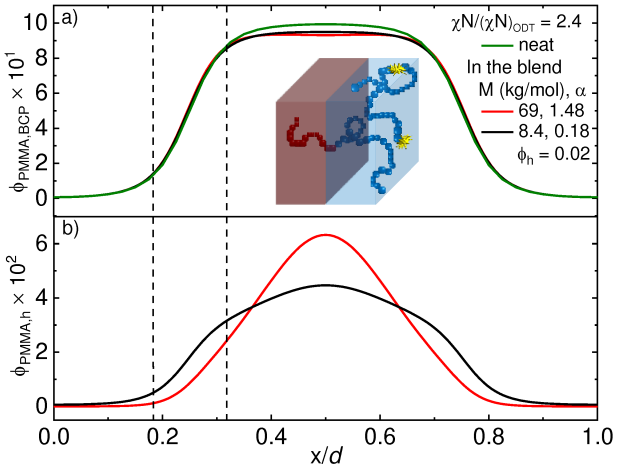

Fig. 1. a) Local volume fraction (segment density) profiles of PMMA segments belonging to the diblock copolymer ($\phi_{PMMA,BCP}$), for three different cases, all with the diblock $\chi N/(\chi N)_{ODT}$ = 2.4: neat diblock (green), and ϕ_h = 0.02 blends with α = 0.18 (black) and α = 1.48 (red). Dashed vertical lines demarcate the width of the interface. Inset: schematic of a self-assembled lamellar blend of a PBMA-PMMA diblock copolymer and a dilute PMMA-py homopolymer, where the label (yellow) is randomly located along the homopolymer chain. b) Corresponding segment density profiles for PMMA segments belonging to the PMMA-py homopolymer ($\phi_{PMMA,h}$) for the same two blends as in (a).

The structure of the blend of a dilute PMMA-py homopolymer with a symmetric (volume fraction ϕ_{PMMA} = ϕ_{PBMA} = 0.5) lamellar PBMA-PMMA diblock copolymer is schematically shown in the inset of Fig. 1(a). The blend is defined in terms of the segregation strength of the diblock copolymer (χN, where χ represents the Flory interaction parameter, and N the degree of polymerization of the diblock), the volume fraction of a component in the diblock ($\phi_{PMMA,BCP}$), the volume fraction of the

homopolymer in the blend (ϕ_h), and the molecular weight of the homopolymer relative to that of the diblock copolymer ($\alpha = M_h/M_{BCP}$) [20]. For the diblock employed here, M_{BCP} = 47 kg/mol, the domain period d = 27 nm, and $\chi N/(\chi N)_{ODT} \approx 2.4$ [19], where $(\chi N)_{ODT}$ is the segregation strength at the order-disorder transition. The component distributions are quantitatively calculated here via self-consistent field theory (SCFT) [20], using open-source software developed by Arora et al. [21]. The green curve in Fig. 1(a) shows the composition profile of PMMA segments in the neat diblock over one domain period starting in the center of the PBMA-rich domain (x/d = 0 or 1). For blends at ϕ_h = 0.02, the value of d is predicted by SCFT to increase by a maximum of 1.5% at α = 1.48, relative to the neat diblock, a negligible increase in agreement with experiments [22,23]. The interfacial thickness represented by vertical dashed lines in Fig. 1 was previously determined using small angle x-ray scattering [19] on the neat diblock copolymer, and is predicted, by SCFT, to be essentially unaffected by blending with 2 vol% homopolymer. At the α values employed in this work, the PMMA homopolymer strongly partitions into the PMMA-rich domains of the diblock; with increasing α, the homopolymer is more strongly localized in the center of the PMMA domain. These features are quantitatively captured in the SCFT results shown in Fig. 1(b).

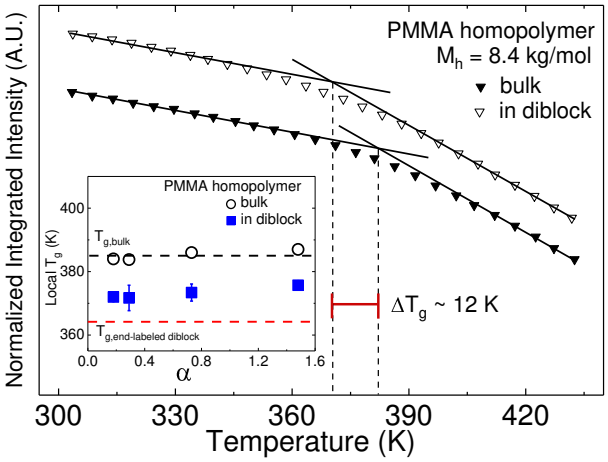

Fig. 2. Temperature dependence of the integrated fluorescence emission intensity and the corresponding linear fits in the glassy and rubbery regions of a PMMA-py homopolymer (M_h = 8.4 kg/mol) either in bulk (solid symbols) or blended at a 2% volume fraction into the unlabeled PBMA-PMMA diblock copolymer. Integrated intensities are normalized to unity at the highest temperature, and shifted vertically in the figure for clarity. Inset: local T_g vs. α for PMMA-py homopolymers in the bulk (open circles, data from [19]) or blended into an unlabeled diblock copolymer (blue squares); error bars indicate ± 1 standard deviation. The dashed black horizontal line is the bulk T_g (385 K) of the PMMA homopolymer at $M_h \cong 20$ kg/mol. The dashed red horizontal line is the T_g (364 K) of a neat PBMA-PMMA diblock copolymer labeled at the chain end [19].

The T_g of the PMMA-py homopolymers of varying M was characterized using temperature-dependent fluorescence spectroscopy according to procedures described previously [19,24]; details are provided in the Supplementary Material. In brief, the total fluorescence emission intensity from the pyrene labels was measured upon cooling

from the melt; a decrease in the slope of the intensity vs. temperature upon transitioning from the melt to the glass signifies T_g. Fig. 2 shows the determination of T_g for the PMMA-py homopolymer with M_h = 8.4 kg/mol (α = 0.18), both neat (filled symbols) and blended into the diblock at ϕ_h = 0.02 (open symbols); the homopolymer T_g in the blend is depressed by 12 K relative to its bulk value. A similar trend is observed at all values of α as shown in the inset of Fig. 2; the four homopolymers in bulk show an average T_g = 385 K, weakly increasing with M_h [19], while the same homopolymers show an average T_g = 373 K in the dilute blends. However, T_g for the PMMA blocks in the neat diblock is lower still: for a PBMA-PMMA diblock selectively labeled at the PMMA chain end, which shows a labeled segment density profile comparable to the homopolymer profiles in Fig. 1(b), T_g = 364 K [19]. Thus, Fig. 2 conveys the surprising result that the PMMA homopolymer dynamics in the blend appear to be slower ($T_g \approx$ 373 K) than those of neighboring PMMA segments from the diblock chains ($T_g \approx$ 364 K), which are attached to the PBMA-PMMA domain interface.

To properly gauge the impact of block connectivity across the domain interface, three factors which can influence T_g need to be considered: 1) segmental mixing (*i.e.*, plasticization of PMMA segments by PBMA segments, when $\phi_{PMMA} < 1$ locally), 2) depression of the PMMA T_g through soft confinement [25] by the PBMA domains, analogous to T_g depression by a free surface [17,26], and 3) the influence of block connectivity, *i.e.*, whether the PMMA segments being probed are covalently bound to a PBMA block (and therefore to the domain interface) or not. In the neat diblock case, examined previously [19], factors #2 and #3 are inextricably combined, since all PMMA

blocks are connected to PBMA blocks. However, in the present work, comparison of the neat diblock and dilute homopolymer blend cases allows these effects to be separated.

The first of these three factors, segmental mixing, can be captured through the well-known Fox equation [27], eqn. (1), while also accounting for the local self-concentration [12] of PMMA segments due to chain connectivity through eqn. (2):

$$\frac{1}{T_g(\phi_{eff,PMMA})} = \frac{\phi_{eff,PMMA}}{T_{g,PMMA}} + \frac{1-\phi_{eff,PMMA}}{T_{g,PBMA}} \qquad (1)$$

$$\phi_{eff,PMMA} = \phi_s + (1-\phi_s)\phi_{PMMA} \qquad (2)$$

In eqn. (2), ϕ_{PMMA} is the local volume fraction of PMMA segments at any point within the domain structure, while ϕ_s is the self-concentration of PMMA segments. Previous measurements [19] have shown that eqns. (1) and (2) satisfactorily describe the T_g in disordered PBMA-PMMA diblocks, wherein the two blocks are intimately mixed, with ϕ_s = 0.38. The expected T_g, if segmental mixing were the only effect operative, is then calculated by linearly weighting the local T_g calculated from eqns. (1) and (2) by the labeled segment distribution obtained from SCFT (see Supplemental Material [28] Fig. S4 and [19]). The T_g so calculated for the diblock labeled at the PMMA end is 378 K [19], only ~7 K below the T_g of bulk PMMA and much higher than the observed T_g = 364 K. Thus, as previously noted [19], segmental mixing makes only a modest contribution to the PMMA T_g depression observed in the neat diblock; the dominant factors are soft confinement and/or block connectivity, but these two cannot be separated in the neat diblock.

To isolate the effect of block connectivity, the T_g values measured on the dilute blends in Fig. 2 should be compared with the T_g measured on a selectively-labeled neat

diblock having exactly the same labeled segment density distribution; in this way, both segmental mixing and the effect of soft confinement are exactly matched between the two cases, since the labeled segments are in precisely the same distribution of environments, and at the same distribution of distances from the PBMA-PMMA domain interface. Fig. 3(a) shows the SCFT-calculated labeled segment density distributions for two different label positions in the neat diblock: 20% and 72% of the distance along the PMMA block (J+20 and J+72) from the block junction (J). For comparison, the labeled segment density distributions for the $\alpha = 0.29$ and $\alpha = 0.73$ blends are shown as dashed curves. Amongst all possible label positions in the diblock, J+72 corresponds to the narrowest calculated segment density distribution (most strongly localized in the PMMA domain center); for label positions beyond 72% of the PMMA block length, the additional conformational freedom associated with the chain end actually broadens the distribution [6]. Experimentally, a PBMA-PMMA diblock ($(\chi N)/(\chi N)_{ODT} \approx 2.4$) labeled at J+72 shows $T_g = 364 \pm 3$ K (one standard deviation) by fluorimetry (see Supplemental Material [28] Fig. S2(a)). The $\alpha = 0.29$ blend has a similar labeled segment density distribution to J+72, but an experimental $T_g = 372 \pm 4$ K. This difference reflects the effect of block connectivity: an 8 K (±5 K) depression of the PMMA T_g by tethering it to a PBMA block (in the diblock) vs. having it "float free" within the PMMA domain (in the blend).

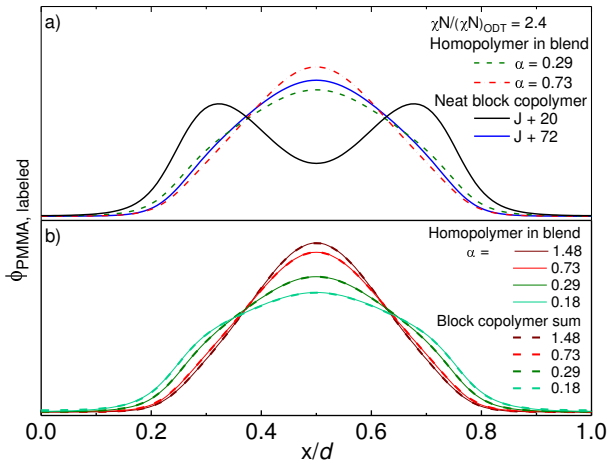

Fig. 3. (a) Segment density profiles across one domain period for two label positions in the diblock copolymer (solid lines), or labeled homopolymer segments in the ϕ_h = 0.02 blend at two values of α (dashed lines), across one domain period. All profiles are normalized to equal area. (b) Normalized segment density profiles for the four labeled homopolymers (varying α), all in blends at ϕ_h = 0.02 (solid curves). The dashed curve superimposed on each solid curve represents the best-fit weighted sum of the labeled segment density profiles in the neat diblock ($\chi N/(\chi N)_{ODT}$ = 2.4), corresponding to six discrete label positions along the PMMA block.

To make a similar comparison for the other values of α, the labeled segment density distributions for six different label positions in the neat diblock (J+20 and J+72, shown in Fig. 3(a), plus J, J+5, J+50, and J+100 (end-labeled) from [19]) were summed, with weights adjusted to match the sum to the homopolymer's segment density distribution in the blend. Applying these same weights to the measured values of T_g for each selectively-labeled diblock was previously demonstrated to satisfactorily reproduce the T_g for PBMA-PMMA diblocks where the label was uniformly distributed along the

PMMA block [19]. For the α = 0.73 and α = 1.48 cases, since the homopolymer segment density distribution is narrower than the narrowest block copolymer distribution (J+72), the J+20 profile—which has most of its segments just beyond the interface (see Fig. 3(a))—needed to be accorded a negative weight (see Supplemental Material [28] for details). Fig. 3(b) compares the homopolymer segment densities with the best-fit weighted sums of the labeled diblock segment densities; an excellent match is achieved in all cases.

Fig. 4 captures and separates the three aforementioned effects quantitatively. Each blend is characterized on the abscissa by the average distance (z) of the labeled segments from the nearest interface (at *x/d* = 0.25 or 0.75 in Fig. 3(b)). As α increases, the homopolymer segments become progressively more localized in the domain center, so z increases monotonically with α. The experimental T_g values for the labeled homopolymers in the blends are shown as the blue squares. The black (filled) circles represent the T_g values expected simply from segmental mixing (effect #1, calculated locally according to eqns. (1) and (2) and averaged across the homopolymer's segment density profile). Segmental mixing produces a modest 4-9 K depression in T_g relative to the value for bulk PMMA (385 K), with the magnitude of the depression decreasing with increasing z (increasing localization of the homopolymer in the PMMA-rich domain center). The white (open) triangles represent the T_g values calculated by applying the weights obtained from the summation in Fig. 3(b) to the experimentally measured T_g values [19] for the selectively-labeled diblocks; these calculated values should incorporate the contributions from all three effects. Recall that the J+72 labeled diblock showed T_g = 364 K; the open symbols in Fig. 4 naturally bracket this value. At low α,

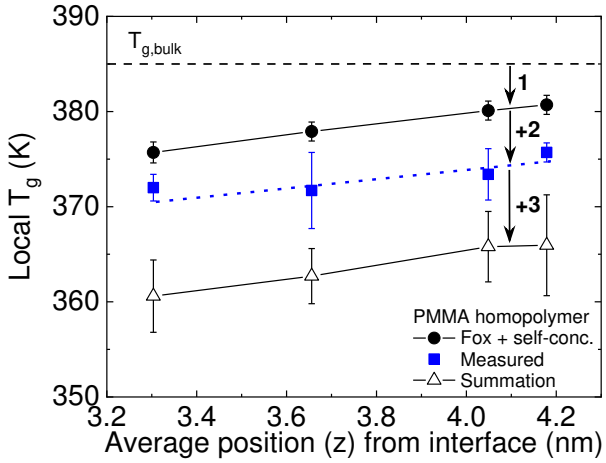

Fig. 4. Local T_g for the four PMMA-py homopolymers in ϕ_h = 0.02 blends with the diblock (blue squares; dashed blue curve is guide to the eye) plotted against the average distance (z) of the homopolymer segments from the nearest PBMA-PMMA domain interface. For comparison, the T_g values calculated simply from segmental mixing (via eqns. (1) and (2)) are shown as the filled circles, while the T_g values calculated for a selectively labeled diblock, having the same labeled segment density distribution as the homopolymer, are shown as the open triangles; the uncertainties in T_g are propagated from the uncertainties in the T_g values uses as inputs to the calculations. Comparison of the three curves reveals the magnitude of each of the three effects contributing to T_g depression in nanostructured block copolymers: 1) segmental mixing, 2) soft confinement, and 3) block connectivity across the domain interface.

where the homopolymer segment density distribution is broader than J+72 (Fig. 3(a)), T_g < 364 K for the sum of the block copolymer segment density distributions, because of both enhanced segmental mixing (more labeled PMMA segments in interfacial region), and stronger soft confinement (smaller z, labeled PMMA segments closer on average to PBMA domain); conversely, at high α, both segmental mixing and the proximity to the

interface are reduced, and T_g > 364 K. But these effects are modest; the average T_g represented by the four open triangles in Fig. 4 is 363 K, far below the average experimental value (blue points) of T_g = 373 K for labeled homopolymers in diblock matrices.

From top to bottom, the three sets of points in Fig. 4 progressively incorporate the three effects alluded to above. The black symbols consider only segmental mixing (effect #1), which produces a 4-9 K depression relative to the bulk PMMA T_g = 385 K. The experimental (blue) points contain contributions from both segmental mixing and confinement (effects #1 and #2); confinement therefore produces an additional reduction in T_g of approximately 5 K (the black and blue curves are parallel to within the experimental uncertainty, indicating that the principal effect of varying α is to change the extent of segmental mixing). Finally, the open symbols incorporate all three effects (segmental mixing, confinement, and block connectivity), because they are calculated for a selectively labeled diblock (in which all three effects are present) having the same labeled segment density distribution as the homopolymer in the blend. Block connectivity (effect #3) is thus seen to produce an additional T_g depression of ~ 10 K. In other words—and quite unexpectedly—attachment of the PMMA block to the PBMA block, and thereby to the domain interface, produces a larger T_g depression than either confinement by the domain structure or segmental mixing.

The results obtained here complement previous studies of homopolymers in hard confinement, where a substantial increase in the local T_g was observed by covalently bonding (grafting) polymer chains to a solid substrate vs. simply coating the polymer onto the same weakly-interacting substrate [32-34], or when the polymer layer being

probed rests atop a grafted brush layer attached to a hard substrate [35-37]. The present study highlights the utility of fluorescence labeling and temperature-dependent spectroscopy, which provide component-specific measurements of T_g, to probe features of the glass transition in complex polymer systems. In the present case, this approach reveals that even in intimate blends, neighboring—and chemical identical—segments (PMMA here) can exhibit different local dynamics when attached to a chemically-distinct—and distant—block (PBMA here).

Acknowledgments: This work was supported by the National Science Foundation (NSF) Materials Research Science and Engineering Center Program through the Princeton Center for Complex Materials (DMR-1420541). D.C. acknowledges the support of an NSF graduate research fellowship. R.D.P. acknowledges the AFOSR through a PECASE Award (FA9550-12-1-0223).

References

1. L. Leibler, Macromolecules **13**, 1602 (1980).
2. M. W. Matsen and F. S. Bates, Macromolecules **29**, 1091 (1996).
3. A. M. Mayes, T. P. Russell, S. K. Satija, and C. F. Majkrzak, Macromolecules **25**, 6523 (1992).
4. M. W. Matsen, Phys. Rev. Lett. **74**, 4225 (1995).
5. Y. Miwa, K. Yamamoto, T. Tanabe, S. Okamoto, M. Sakaguchi, M. Sakai, and S. Shimada, J. Phys. Chem. B **110**, 4073 (2006).
6. K. R. Shull, A. M. Mayes, and T. P. Russell, Macromolecules **26**, 3929 (1993).
7. J. Colmenero and A. Arbe, Soft Matter **3**, 1474 (2007).
8. J. A. Pathak, R. H. Colby, S. Y. Kamath, S. K. Kumar, and R. Stadler, Macromolecules **31**, 8988 (1998).
9. J. A. Pathak, R. H. Colby, G. Floudas, and R. Jérôme, Macromolecules **32**, 2553 (1999).
10. J. C. Haley and T. P. Lodge, Colloid Polym. Sci. **282**, 793 (2004).
11. J. A. Zawada, G. G. Fuller, R. H. Colby, L. J. Fetters, and J. Roovers, Macromolecules **27**, 6861 (1994).
12. T. P. Lodge and T. C. B. McLeish, Macromolecules **33**, 5278 (2000).
13. R. P. Sharma and P. F. Green, Macromolecules **50**, 6617 (2017).
14. Y. Y. He, T. R. Lutz, and M. D. Ediger, J. Chem. Phys. **119**, 9956 (2003).
15. L. Willner, R. Lund, M. Monkenbusch, O. Holderer, J. Colmenero, and D. Richter, Soft Matter **6**, 1559 (2010).

16. V. Sethuraman, V. Pryamitsyn, and V. Ganesan, J. Polym. Sci. B Polym. Phys. **54**, 859 (2016).

17. J. A. Forrest, K. Dalnoki-Veress, J. R. Stevens, and J. R. Dutcher, Phys. Rev. Lett. **77**, 4108 (1996).

18. C. Zhang, Y. L. Guo, and R. D. Priestley, Macromolecules **44**, 4001 (2011).

19. D. Christie, R. A. Register, and R. D. Priestley, ACS Cent. Sci. **4**, 504 (2018).

20. M. W. Matsen, Macromolecules **28**, 5765 (1995).

21. A. Arora, J. Qin, D. C. Morse, K. T. Delaney, G. H. Fredrickson, F. S. Bates, and K. D. Dorfman, Macromolecules **49**, 4675 (2016).

22. H. Tanaka, H. Hasegawa, and T. Hashimoto, Macromolecules **24**, 240 (1991).

23. M. P. Stoykovich, E. W. Edwards, H. H. Solak, and P. F. Nealey, Phys. Rev. Lett. **97,** 147802 (2006).

24. C. J. Ellison and J. M. Torkelson, J. Polym. Sci. B Polym. Phys. **40**, 2745 (2002).

25. C. B. Roth and J. R. Dutcher, Eur. Phys. J. E **12**, S103 (2003).

26. R. J. Lang, W. L. Merling, and D. S. Simmons, ACS Macro Lett. **3**, 758 (2014).

27. T. G. Fox, Bull. Am. Phys. Soc. **1**, 123 (1956).

28. See Supplemental Material at [URL] for a detailed description of the experimental methods, which includes Refs. [29-31], as well as discussion of the definition of α, and of negative weights applied to the segment density distributions.

29. C. J. Ellison and J. M. Torkelson, Nat. Mater. **2**, 695 (2003).

30. S. K. Varshney, J. P. Hautekeer, R. Fayt, R. Jérôme, and P. Teyssié, Macromolecules **23**, 2618 (1990).

31. R. A. Orwoll, in *Physical Properties of Polymers Handbook*, 2nd edition, edited by J. E. Mark (Springer Science+Business Media, New York, 2007), p. 93.

32. R. S. Tate, D. S. Fryer, S. Pasqualini, M. F. Montague, J. J. de Pablo, and P. F. Nealey, J. Chem. Phys. **115**, 9982 (2001).

33. H. N. Wang, J. L. Hor, Y. Zhang, T. Y. Liu, D. Lee, and Z. Fakhraai, ACS Nano **12**, 5580 (2018).

34. T. Lan and J. M. Torkelson, Polymer **64**, 183 (2015).

35. G. Uğur, B. Akgun, Z. Jiang, S. Narayanan, S. Satija, and M. D. Foster, Soft Matter **12**, 5372 (2016).

36. X. R. Huang and C. B. Roth, ACS Macro Lett. **7**, 269 (2018).

37. H. Lee, V. Sethuraman, Y. Kim, W. Lee, D. Y. Ryu, and V. Ganesan, Macromolecules **51**, 4451 (2018).